

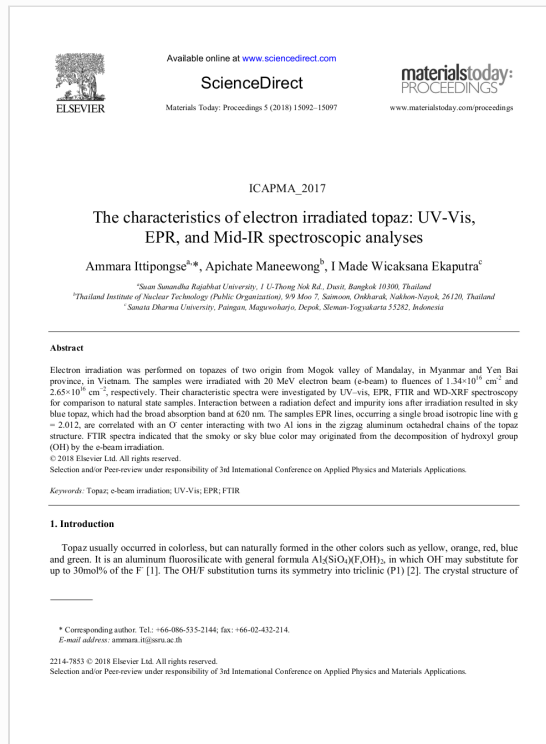


## Digital Receipt

This receipt acknowledges that **Turnitin** received your paper. Below you will find the receipt information regarding your submission.

The first page of your submissions is displayed below.

Submission author: I Made Wicaksana Ekaputra  
Assignment title: Periksa similarity  
Submission title: The characteristics of electron irradiated topaz UV-Vis, EPR, ...  
File name: adiated\_topaz\_UV-Vis,\_EPR,\_and\_Mid-IR\_spectroscopic\_analy...  
File size: 644.2K  
Page count: 6  
Word count: 2,712  
Character count: 14,154  
Submission date: 31-Jan-2023 09:50AM (UTC+0700)  
Submission ID: 2003001050



# The characteristics of electron irradiated topaz UV-Vis, EPR, and Mid-IR spectroscopic analyses

*by* Ekaputra I Made Wicaksana

---

**Submission date:** 31-Jan-2023 09:50AM (UTC+0700)

**Submission ID:** 2003001050

**File name:** adiated\_topaz\_UV-Vis,\_EPR,\_and\_Mid-IR\_spectroscopic\_analyses.pdf (644.2K)

**Word count:** 2712

**Character count:** 14154

ICAPMA\_2017

## The characteristics of electron irradiated topaz: UV-Vis, EPR, and Mid-IR spectroscopic analyses

Ammara Ittipongse<sup>a,\*</sup>, Apichate Maneewong<sup>b</sup>, I Made Wicaksana Ekaputra<sup>c</sup><sup>a</sup>*Suan Sunandha Rajabhat University, 1 U-Thong Nok Rd., Dusit, Bangkok 10300, Thailand*<sup>b</sup>*Thailand Institute of Nuclear Technology (Public Organization), 9/9 Moo 7, Saimoon, Onkharak, Nakhon-Nayok, 26120, Thailand*<sup>c</sup>*Sanata Dharma University, Paingan, Maguwaharjo, Depok, Sleman-Yogyakarta 55282, Indonesia*

### Abstract

Electron irradiation was performed on topazes of two origin from Mogok valley of Mandalay, in Myanmar and Yen Bai province, in Vietnam. The samples were irradiated with 20 MeV electron beam (e-beam) to fluences of  $1.34 \times 10^{16} \text{ cm}^{-2}$  and  $2.65 \times 10^{16} \text{ cm}^{-2}$ , respectively. Their characteristic spectra were investigated by UV-vis, EPR, FTIR and WD-XRF spectroscopy for comparison to natural state samples. Interaction between a radiation defect and impurity ions after irradiation resulted in sky blue topaz, which had the broad absorption band at 620 nm. The samples EPR lines, occurring a single broad isotropic line with  $g = 2.012$ , are correlated with an O<sup>•</sup> center interacting with two Al ions in the zigzag aluminum octahedral chains of the topaz structure. FTIR spectra indicated that the smoky or sky blue color may originated from the decomposition of hydroxyl group (OH) by the e-beam irradiation.

© 2018 Elsevier Ltd. All rights reserved.

Selection and/or Peer-review under responsibility of 3rd International Conference on Applied Physics and Materials Applications.

**Keywords:** Topaz; e-beam irradiation; UV-Vis; EPR; FTIR

### 1. Introduction

Topaz usually occurred in colorless, but can naturally formed in the other colors such as yellow, orange, red, blue and green. It is an aluminum fluorosilicate with general formula  $\text{Al}_2(\text{SiO}_4)(\text{F},\text{OH})_2$ , in which OH<sup>-</sup> may substitute for up to 30mol% of the F<sup>-</sup> [1]. The OH/F substitution turns its symmetry into triclinic (P1) [2]. The crystal structure of

\* Corresponding author. Tel.: +66-086-535-2144; fax: +66-02-432-214.

E-mail address: [ammara.it@ssru.ac.th](mailto:ammara.it@ssru.ac.th)

topaz is  $\text{Al}_2\text{SiO}_5$  long to the orthorhombic with space group  $\text{Pbnm}$  ( $\text{D}_{2h}^{16}$ ) [3] and four molecules per unit cell. Its structure consists of chains of a pair of edge-shared  $\text{AlO}_4\text{F}_2$  octahedra and corner-shared  $\text{SiO}_4$  tetrahedra that linking octahedral chains in a zigzag fashion parallel to the crystalline c-axis. Topaz is most commonly irradiated with a variety of radiations. Sky blue color, a light pure blue color, can produce by exposure the white topaz to gamma rays and continue by heating it to burn off undesired brown overtones that appear during the exposure process. On the other hand, if exposure the white topaz to neutrons in a research reactor and /or electrons in a linear electron accelerator will produce the darker shades which we know as London blue and Swiss blue.

The coloration of topaz is frequently governed by transition metal impurities or by irradiation. Many authors has been attributed the blue color to an  $\text{O}^-$  defect, produced by irradiation and located in  $\text{OH}^-$  positions of topaz structure, interacting with two equivalent structural Al ions [4-5]. The  $\text{O}^-$  defect is related to the absorption band at 620 nm. Some authors have been ascribed this absorption band to the presence of  $\text{Cr}^{3+}$ ,  $\text{Fe}^{2+}$  and  $\text{Mn}^{2+}$  impurities [6-7]. Irradiation treatment caused exchange interaction between these impurities and radiation defect. The chemical composition, different valence states, and occupancy in each site of the topaz structure appear to be associated with one another in the color change caused by irradiation treatment. However, disagreement exists over the detailed origins of the colors. Specifically, the reason for the color changes after e-beam irradiation is still unclear and not well understood.

In the present work, we used Ultraviolet–visible Spectroscopy (UV-Vis), including Wavelength Dispersive X-ray Fluorescence (WDXRF), Electron Paramagnetic Resonance (EPR) measurement and Fourier-transform infrared (FTIR) spectroscopy analyses to study the chemical behaviours of two topaz samples, one originated from Mogok valley of Mandalay, in Myanmar and the other from Yen Bai province, in Vietnam, by e-beam irradiation with two different fluence levels to understand the color change mechanism. We discuss the color change mechanism in relation to e-beam irradiation in terms of the initial point of the jewellery manufacturing process.

## 2. Materials and methods

Natural colorless topaz of two origin in Mogok valley of Mandalay, in Myanmar and Yen Bai province, in Vietnam were investigated. Each sample was cut in half perpendicular to the crystallographic c-axis. Subsequently, all samples are polished by silicon carbide abrasive paper. After cutting and polishing, the samples thickness was in the range of 2.1–3.2 mm. The samples were irradiated with 10 kW power and 20 MeV electrons to fluences of  $4 \times 10^{16} \text{ cm}^{-2}$  and  $2.65 \times 10^{16} \text{ cm}^{-2}$ , respectively. The linear electron accelerator used in this study is located at Gems Irradiation Center, Thailand Institute of Nuclear Technology (TINT) and can produce high energy 5-20 Million Volts (MeV) high power 10-20 kilo Watt (kW). The chemical compositions of the samples were recorded by using the S8 TIGER high-end wavelength dispersive X-ray fluorescence (WDXRF) spectrometer. The spectrometer was installed at the TINT's Service Center. The samples were excited by X-rays (Rh tube) with the power of 50 kW and the current of 50 mA. The optical absorption spectra were measured on the platelets oriented perpendicular to the c-axis before and after irradiation by using the PerkinElmer lambda 750 UV/Vis/NIR spectrophotometer located at the Gems Irradiation Center, Ongkharak Branch, TINT. The wavelength for the optical spectra collected was recorded from 300 to 800 nm by setting a spectral resolution of 2.0 nm with a scan speed of 250 nm/min. All EPR measurements were performed at room temperature on a Bruker EPR spectrometer (ESP 900 series) operated at an X-band microwave frequency at Department of Physics, Sanata Dharma University. The spectrometer's operating conditions adopted during the experiment were a 350.0-mT central magnetic field, a 140- to 600-mT scan ranges, a 9.64-GHz microwave frequency, a 1.0-mW microwave power, a 100-kHz field modulation frequency, a 1.0-mT field modulation amplitude and a 0.02-s time constant. 1, 1-diphenyl-2-picrylhydrazyl (DPPH) with a g factor of 2.0036 was used as an internal standard for g-factor calculations. After the spectra had been measured, the positions of the EPR signals were labelled by using their effective g ( $g_{\text{eff}}$ ) values. The  $g_{\text{eff}}$  was calculated by using the relationship,  $g_{\text{eff}} = h\nu/\beta H$ , where  $h$ ,  $\nu$ ,  $\beta$ , and  $H$  are Planck's constant, the microwave frequency, the electron Bohr magneton and the external field, respectively. The line width ( $\Delta B_{\text{pp}}$ ) of each signal was also observed. The mid-infrared spectra of the samples were recorded in the region of 400-5000  $\text{cm}^{-1}$  by using a Bruker ALPHA Spectrometer with a resolution of 4  $\text{cm}^{-1}$  at the Department of Mineral Resources under the Ministry

of Natural Resources and Environment, Thailand. Band fittings were done with Gauss- Lorentz functions by using the fitting program OriginPro 2015.

### 3. Results and discussion

The chemical analyses of a given samples obtained by WDXRF were listed in table 1. The WDXRF analysis indicated that both samples were topaz pegmatite. The analyzed topazes reveal a low Fe content and minor amounts of Na, Mg, Br, and Rb, while Cs are present about two time (0.69wt%/0.27wt%) higher in the topaz originated from Mogok valley (M) than the topaz from Yen Bai province (V). In M also present minor quantities of Ni and Ti higher than in V. Other contents, such as Cr and Cu, were detected in subordinate concentrations. There is no significant difference of both samples. In the same way, the correlation of color is not related to chemical composition.

Table 1 Chemical composition of the two topaz samples as measured by using WDXRF analyses.

	Mogok valley (M)	Yen Bai province (V)
Oxide: wt%		
Al <sub>2</sub> O <sub>3</sub>	59.47	59.49
SiO <sub>2</sub>	37.47	37.40
Na <sub>2</sub> O	0.97	1.44
MgO	1.16	1.30
Fe <sub>2</sub> O <sub>3</sub>	0.02	0.04
Br <sub>2</sub> O	0.08	0.01
Rb <sub>2</sub> O	0.04	0.03
Cs <sub>2</sub> O	0.69	0.27
Oxide: wt ppm		
CuO	41	40
Ni <sub>2</sub> O <sub>3</sub>	413	33
TiO <sub>2</sub>	133	52
Total	99.96	99.98

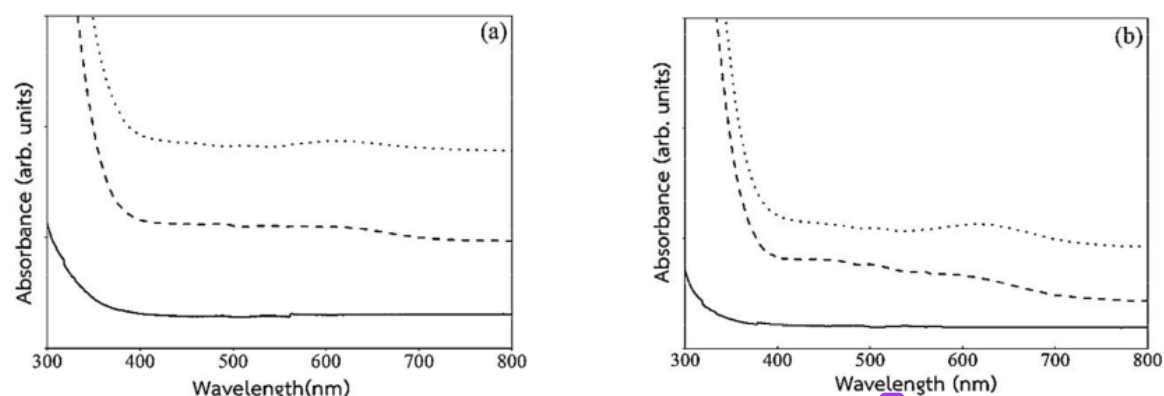


Fig. 1. UV-Vis spectra of (a) M and (b) V: natural state (solid line), after e-beam irradiations at  $1.34 \times 10^{16} \text{ cm}^{-2}$  (dashed line) and  $2.65 \times 10^{16} \text{ cm}^{-2}$  (dotted line).



The UV-Vis absorption spectra (E<sub>⊥c</sub>) of the colorless topaz before irradiation (solid line), after e-beam irradiations at  $1.34 \times 10^{16} \text{ cm}^{-2}$  (dashed line) and  $2.65 \times 10^{16} \text{ cm}^{-2}$  (dotted line) are given in Fig. 1. The natural colorless topazes exhibited no absorption band in both specimens. After e-beam irradiation at  $1.34 \times 10^{16} \text{ cm}^{-2}$ , both samples appear a broad band with maxima at 620 nm and this band increased the intensity, after add the level of e-beam irradiation up to  $2.65 \times 10^{16} \text{ cm}^{-2}$ , resulting in the crystals obtained pale (sky) blue color.

The blue color in topaz can produced by exposure the colorless topaz to gamma ray, neutron and electron. The detail origin of blue color by each irradiation method are difference. The e-beam irradiation lead to appearing of broad band at 620 nm ascribed to the presence of  $\text{Cr}^{3+}$ ,  $\text{Fe}^{2+}$  and  $\text{Mn}^{2+}$  impurities by many authors [6, 7]. Because both topazes have no Mn ions (Table 1) and any other absorption peak for  $\text{Cr}^{3+}$  and  $\text{Fe}^{2+}$ , one possible reason for the appearance of the absorption band at around 620 nm may be the  $\text{O}^-$  defect, as suggested in a previous work based on the results obtained by using e-beam irradiation [8].

Fig. 2 shows the EPR spectra of both e-beam irradiated topazes for the magnetic field perpendicular to the c-axis. The paramagnetic defects are observed in the same position after electron irradiation. The spectra exhibited an intense broad resonance signal at  $g \sim 2.012$  with peak-to-peak line width of  $\sim 14.20 \text{ mT}$ . This resonance signal is the  $\text{O}^-$  hole center, which has been identified as an  $\text{O}^-$  ion on an  $(\text{OH})^-$  site having resolved hyperfine interactions with two equivalent nearest  $\text{Al}^{3+}$  ions [9]. After e-beam irradiation, the both topazes shows the peroxy radical  $\text{O}_2^-$  [10, 11] responded to the broad isotropic resonance line. It is observe that the EPR lines at  $g \sim 2.012$  increased the intensity when the electrons fluence level rising up.

The OH stretching and bending modes of topaz response in three regions,  $600\text{--}1200 \text{ cm}^{-1}$ ,  $2500\text{--}3800 \text{ cm}^{-1}$ ,  $4700\text{--}4900 \text{ cm}^{-1}$ , of mid-infrared (Mid-IR) spectra. In the  $600\text{--}1200 \text{ cm}^{-1}$  region are occasionally appears for the OH bending mode in crystal together with OH stretching mode [12]. However, the absorption peaks of OH bending mode in minerals are difficult to assign, due to this wavenumber region is overlapped by Si-O or Al-O fundamental mode of minerals. Next, the OH stretching modes are produced strong absorption in the  $2500\text{--}3800 \text{ cm}^{-1}$  region [13]. The final region,  $4700\text{--}4900 \text{ cm}^{-1}$ , is assigned to a combination of OH stretching and bending modes [14].

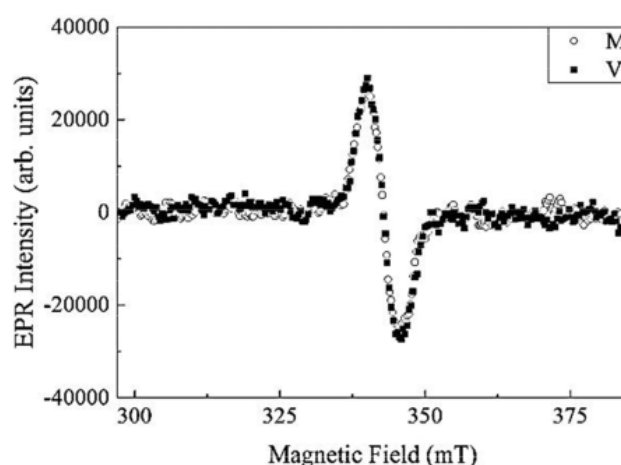


Fig. 2. EPR Spectra of M (circle-symbol line) and V (square-symbol line).

In Fig. 3, the Mid-IR spectra of the topaz samples, M and V, obtained from the Department of Mineral Resources are shown. The spectra of all two samples in their natural states (solid line) were rather similar. M showed a negligible spectra intensity than V throughout the Mid-IR region. The weak bands appeared in range  $4780\text{--}4830 \text{ cm}^{-1}$  with the peak at  $4800 \text{ cm}^{-1}$ , and strong intensity bands appeared in range from  $3610\text{--}3690 \text{ cm}^{-1}$  with the peak at  $3650 \text{ cm}^{-1}$ . The  $4800 \text{ cm}^{-1}$  absorption band is defined as combination of OH stretching and bending modes, while the  $3650 \text{ cm}^{-1}$  absorption band is assigned to OH stretching modes. The low wavenumber region which referred to OH bending mode cannot observed in both topaz samples. All samples exhibited similar

6

behaviors, decreasing in the intensity of absorption bands at  $3650\text{ cm}^{-1}$  and  $4800\text{ cm}^{-1}$  after e-beam irradiation (dashed and dotted line). The decomposing by electron of the  $\text{OH}^-$  groups into  $\text{O}^-$  (hole trap) and  $\text{H}^0$  (electron trap) resulted in a decrease of the intensity.

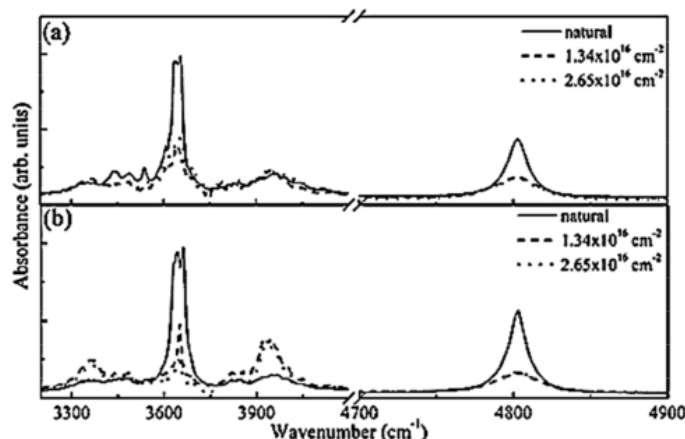


Fig. 3. Mid-infrared spectra in the  $3300 - 4900\text{ cm}^{-1}$  region for (a) M and (b) V: natural state (solid line), after e-beam irradiations at  $1.34 \times 10^{16}\text{ cm}^{-2}$  (dashed line) and  $2.65 \times 10^{16}\text{ cm}^{-2}$  (dotted line).

#### 4. Conclusion

Colorless topazes with different chemical composition changed to a pale blue color after e-beam irradiation. Therefore, the absorption bands at  $620\text{ nm}$  were observed. This band is correlated with the creation of  $\text{O}^-$  defect by electron which supported by EPR spectra. The EPR signal at  $g \sim 2.012$  which has been identified as an  $\text{O}^-$  ion on an  $(\text{OH})^-$  site increased the intensity when the electrons fluency level rising up. Decomposing of  $\text{OH}^-$  groups are occurred after e-beam irradiation from evidence of Mid-IR spectra. Furthermore, decomposing of  $\text{OH}^-$  groups are occurred after e-beam irradiation from evidence of Mid-IR spectra. The absorption bands at  $3650\text{ cm}^{-1}$  and  $4800\text{ cm}^{-1}$  after e-beam irradiation indicated OH stretching modes and combination of OH stretching and bending modes, respectively.

#### Acknowledgments

The authors would like to thank Sterigenics (Thailand) Co., Ltd. for providing the samples. In addition, for sample preparations and WDXRF analyses, we are grateful to Chanida Makakum, Panyanuch Adisak, the head of the radiation machine management division at the Gems Irradiation Center, Thailand Institute of Nuclear Technology (TINT), including staff members, namely, Saruda Panomwong, Nongnuch Jangsawang, and Tasanee Charoenam, is to provide the indispensable process of electron beam irradiation.

#### References

- [1] Y. Song, X. Yuan, New method for identification of blue topaz – an application of cathodoluminescence (CL), *J. Geogr. Geol.* 1(2) (2009) 13-19.
- [2] Pinheiro M. V. B., Fantini C., Krambrock K., Persiano A. I. C., Dantas M. S. S., Pimenta M. A., OH/F substitution in topaz studied by Raman spectroscopy, *Phys. Rev. B* 65 (2002) 104301-6.
- [3] Northrup, P. A.; Leinenweber, K.; Parise, J. B., The location of H in the high-pressure synthetic  $\text{Al}_2\text{SiO}_4(\text{OH})_2$  topaz analogue Sample OH synthetic, *Am. Mineral.* 79 (1994) 401-04.
- [4] A.S. Leal, K. Krambrock, L.G.M. Ribeiro, M.Â.B.C. Menezes, P. Vermaercke, L. Sneyers, Study of neutron irradiation-induced colors in Brazilian topaz, *Nucl. Instr. Meth. Phys. Res. A* 580 (2007) 423–26.
- [5] K. Krambrock, L. G. M. Ribeiro, M. V. B. Pinheiro, A. S. Leal, M. Â. B. C. Menezes, J.M. Spaeth, Color centers in topaz: comparison between neutron and gamma irradiation, *Phys. Chem. Minerals.* 34 (2007) 437–44.

- [6] V. Skvortsova, N. Mironova- Ulmane, L. Trinkler, G. Chikvaidze, Optical properties of natural topaz, IOP Conf. Series: Mater. Sci. Eng. 49 (2013) 012051:1-4.
- [7] V. Skvortsova, N. Mironova- Ulmane, L. Trinkler, Optical Properties of Irradiated Topaz Crystals, IOP Conf. Ser.: Mater. Sci. Eng. 80 (2015) 012008:1-5.
- [8] S. Shin, J. Seo, H. Park, J. Park, Spectroscopic characteristics of topaz: The impact of electron beam irradiation and heat treatment, J. Ceram. Process. Res. 16 (2014) 89-92.
- [9] D.N. da Silva, K.J. Guedes, M.V.B. Pinheiro, J.M. Spaeth, K. Krambrock, The microscopic structure of the oxygen–aluminium hole center in natural and neutron irradiated blue topaz, Phys. Chem. Minerals. 32 (2005) 436–41.
- [10] V. Priest, D.L. Cowan, D.G. Reichel, F.K. Ross, A dangling silicon bond defect in topaz. J. Appl. Phys. 68 (1990) 3035-37.
- [11] V. Priest, D.L. Cowan, H. Yasar, F.K. Ross, ESR, optical absorption, and luminescence studies of the peroxy-radical defect in topaz, Phys. Rev. B 44 (1991) 9877-82.
- [12] J.A. Gadsden, Infrared spectra of minerals and related inorganic compounds, Butterworths, London 1975.
- [13] R. D. Aines, G. R. Rossman, Water in Minerals? A Peak in the Infrared, J. Geophys. Res. 89 (1984) 4059-71
- [14] K. Shinoda, N. Aikawa, IR active orientation of OH bending mode in topaz, Phys. Chem. Minerals. 24 (1997) 551-54.
- [15] D. Rajesh, Y.C. Ratnakaram, M. Seshadri, A. Balakrishna, T. SatyaKrishna, J. Lumin. 132 (2012) 841–849.



# The characteristics of electron irradiated topaz UV-Vis, EPR, and Mid-IR spectroscopic analyses

## ORIGINALITY REPORT

17%

SIMILARITY INDEX

8%

INTERNET SOURCES

15%

PUBLICATIONS

1%

STUDENT PAPERS

## PRIMARY SOURCES

1

[dlutir.dlut.edu.cn](http://dlutir.dlut.edu.cn)

Internet Source

2%

2

Keiji Shinoda, Nobuyuki Aikawa. "IR active orientation of OH bending mode in topaz", Physics and Chemistry of Minerals, 1997

Publication

1%

3

Libertino, S.. "Cluster formation and growth in Si ion implanted c-Si", Materials Science & Engineering B, 20000214

Publication

1%

4

Authit Phakkhawan, Aparporn Sakulkalavek, Siritorn Buranurak, Pawinee Klangtakai et al. "Investigation of Radiation Effect on Structural and Optical Properties of GaAs under High-Energy Electron Irradiation", Materials, 2022

Publication

1%

5

Qiaoli Liu, Junwei Liu, Dayong Lu, Weitao Zheng, Chaoquan Hu. "Structural evolution and dielectric properties of Nd and Mn co-doped BaTiO<sub>3</sub> ceramics", Journal of Alloys and Compounds, 2018

Publication

1%

6	<a href="http://jmmm.material.chula.ac.th">jmmm.material.chula.ac.th</a> Internet Source	1 %
7	Ammara Ittipongse, Idhisak Sridam. "Influencing Cyber Laboratory Conceptual Change Through Laboratory Learning", Procedia - Social and Behavioral Sciences, 2015 Publication	1 %
8	Motohiro Mizuno, Yoji Aoki, Kazunaka Endo, Darius Greenidge. "Local structure analysis of smoky and colorless topaz using single crystal $^{27}\text{Al}$ NMR", Journal of Physics and Chemistry of Solids, 2006 Publication	1 %
9	K. THAMAPHAT, P. LIMSUWAN, S. M. SMITH. "ELECTRON SPIN RESONANCE INVESTIGATION OF FREE RADICALS PRODUCED IN PULVERIZED NON-IRRADIATED SUGAR", International Journal of Modern Physics B, 2012 Publication	1 %
10	<a href="http://www.bruker.com">www.bruker.com</a> Internet Source	1 %
11	<a href="http://www.journal.uestc.edu.cn">www.journal.uestc.edu.cn</a> Internet Source	1 %
12	Zhang, Y.. "Mixing artifacts from the bolus addition of nitric oxide to oxymyoglobin: implications for S-nitrosothiol formation",	<1 %

13

K. Jomová, O. Kysel, J.C. Madden, H. Morris, S.J. Enoch, S. Budzak, A.J. Young, M.T.D. Cronin, M. Mazur, M. Valko. "Electron transfer from all-trans  $\beta$ -carotene to the t-butyl peroxy radical at low oxygen pressure (an EPR spectroscopy and computational study)", Chemical Physics Letters, 2009

Publication

<1 %

14

[doaj.org](http://doaj.org)

Internet Source

<1 %

15

[www.dragon.lv](http://www.dragon.lv)

Internet Source

<1 %

16

Jannoo, Kanokwan, Churapa Teerapatsakul, Adisak Punyanut, and Wanvimol Pasanphan. "Electron beam assisted synthesis of silver nanoparticle in chitosan stabilizer: Preparation, stability and inhibition of building fungi studies", Radiation Physics and Chemistry, 2015.

Publication

<1 %

17

Souza, D.N.. "Thermally stimulated luminescence and EPR studies on topaz", Applied Radiation and Isotopes, 200608

Publication

<1 %

18

J.R. Durig, Joo Lee Min, T.S. Little, M. Dakkouri, Andreas Grünvogel-Hurst.

<1 %

"Spectra and structure of small ring compounds—LX. Raman and infrared spectra, conformational stability, normal coordinate analysis, and ab initio calculations of cyclobutyl acetylene", *Spectrochimica Acta Part A: Molecular Spectroscopy*, 1992

Publication

19

Shamshad, L., G. Rooh, K. Kirdsiri, N. Srisittipokakun, B. Damdee, H.J. Kim, and J. Kaewkhao. "Photoluminescence and white light generation behavior of lithium gadolinium silicoborate glasses", *Journal of Alloys and Compounds*, 2016.

Publication

<1 %

20

Coustenis, A.. "The composition of Titan's stratosphere from Cassini/CIRS mid-infrared spectra", *Icarus*, 200707

Publication

<1 %

21

L.A. Groat, D.J. Turner, R.J. Evans. "Gem Deposits", Elsevier BV, 2014

Publication

<1 %

22

[d-nb.info](http://d-nb.info)

Internet Source

<1 %

23

[pubs.rsc.org](http://pubs.rsc.org)

Internet Source

<1 %

24

[repository.hanyang.ac.kr](http://repository.hanyang.ac.kr)

Internet Source

<1 %

25

Internet Source

&lt;1 %

26

"97–98 Bibliography", Journal of Molecular Structure, 1998

Publication

&lt;1 %

27

Alice Post, Jan Tullis. "The rate of water penetration in experimentally deformed quartzite: implications for hydrolytic weakening", Tectonophysics, 1998

Publication

&lt;1 %

28

Ju Hee Lee, Hyung Goo Kim, Won Jai Lee. "Characterization and tissue incorporation of cross-linked human acellular dermal matrix", Biomaterials, 2015

Publication

&lt;1 %

29

Min-Jung Jung, Mi-Seon Park, Young-Seak Lee. "Effects of E-Beam Irradiation on the Chemical, Physical, and Electrochemical Properties of Activated Carbons for Electric Double-Layer Capacitors", Journal of Nanomaterials, 2015

Publication

&lt;1 %

30

Otto W. Flörke, Heribert Graetsch, Fred Brunk, Leopold Benda et al. "Silica", Wiley, 2000

Publication

&lt;1 %

31

Kloprogge, J.T.. "The effects of synthesis pH and hydrothermal treatment on the

&lt;1 %

# formation of zinc aluminum hydrotalcites", Journal of Solid State Chemistry, 200411

Publication

---

---

Exclude quotes      On

Exclude matches      < 5 words

Exclude bibliography      On